Heptanuclear disk-like $M^{II}_3Ln^{III}_4$ (M=Ni, Co) coordination clusters: synthesis, structures and magnetic properties

Kieran Griffiths,[a] Chris Harding,[a] Vasiliki N. Dokorou,[a] Edward Loukopoulos,[a] Stavroula I. Sampani,[a] Alaa Abdul-Sada,[a] Graham J. Tizzard,[b] Simon J. Coles,[b] Giulia Lorusso,[c] Marco Evangelisti,[c] Albert Escuer*[d] and George E. Kostakis*[a]

Abstract: The synthesis, characterization, crystal structures and magnetic properties of isoskeletal heptanuclear disk-like $M^{II}_3Ln^{III}_4$ coordination clusters with the general formula $[Co^{II}_3Ln^{III}_4(\mu_3\text{-}OH)_6L_6(CF_3SO_3)](CF_3SO_3)_5]$ where Ln= Gd (**2**), Y (**3**) and $[Ni^{II}_3Ln^{III}_4(\mu_3\text{-}OH)_6L_6(CF_3SO_3)](CF_3SO_3)_5]$ where Ln= Dy (**4**), Gd (**5**), Y (**6**) are presented. All the compounds are stable in solution as confirmed by ESI-MS. Magnetic studies were performed for compounds **2**, **4**, **5** and **6** and indicate ferromagnetic coupling while the magnetocaloric properties of **5** are characterized by $-\Delta S_m$ = -15.4 $Jkg^{-1}K^{-1}$ at T = 5.0 K and ΔT_{ad} = 5.9 K at T = 2.3 K, for $\mu_0\Delta H$ = 7 T.

Introduction

3d and/or 4f coordination clusters (CCs) have been of considerable interest in the past few years due to their aesthetically pleasant structures[1–4] and applications.[5–9] These can be synthesized via self-assembly of organic or inorganic ligands, with metal ions, following the hard soft base acid principle.[10] Serendipitous assembly has been the traditional route of synthesis for these types of molecules, not just relying upon the metal ions and coordination modes of ligands, but on a multitude of other factors including concentration, steric effects, solvent, pH and counter anions.[11] These factors can dramatically affect the shape and topology of the final product. More recently, various approaches have been applied to synthesize these molecules in a more predictable manner.[12–14]

The importance of controlling the shape and topology of CCs is highlighted by their extended study as molecular magnetic materials.[15–18] There are many examples of polynuclear CCs displaying interesting magnetic phenomena such as high spin value,[19–22] single-molecule magnet (SMM)[23–28] or magnetocaloric effect (MCE)[29–33] behavior. The combination of 3d and 4f ions has been proposed to be an efficient strategy to reach heterometallic CCs with improved magnetic properties.[34–36] This combination has resulted in a plethora of examples with various 3d metals; $Fe^{II}_2Dy^{III}$,[37] $Co^{II}_2Dy^{III}_2$,[38] $Mn^{II}Dy^{III}_2$,[39] $Ni^{II}_3Ln_3$,[40] $Cr^{III}_2Ln^{III}_2$,[41] and $Cu^{II}_4Dy^{III}_4$.[42] In addition 3d/Gd(III) CCs have been recognized as excellent examples displaying magnetocaloric effect (MCE) behavior.[43] The first of these was a Mn_4Gd_4 CC supported by calix[4]arene.[44] Notable examples experiencing a large MCE effect have been reported including Mn_4Gd_4,[44,45] M_8Gd_4,[46] $Cu_{36}Ln_{24}$[47] and Cu_5Gd_4.[48]

Schiff base ligands are an ideal host to accommodate both 3d and 4f elements and allow them to interact due to their compartmental nature.[49–56] Recently, we reported a number of 3d and 3d/4f CCs synthesized by the employment of the Schiff base ligand (E)-4-(2-hydroxy-3-methoxy-benzylideneamino)-2,3-dimethyl-1-phenyl-1,2-dihydropyrazol-5-one (H**L1**, Scheme 1).[57–59] The use of H**L1** in Co/Ln cluster chemistry has afforded a series of Co^{II}/Dy^{III} CCs with various nuclearities (4-8).[57,59] Among these compounds the heptanuclear disk-like CC formulated $[Co^{II}_3Dy^{III}_4(\mu_3\text{-}OH)_6(\mathbf{L1})_6(CF_3SO_3)]$ $(ClO_4)_5$ (**1**) displays behavior indicative of an SMM below 4K.[57]

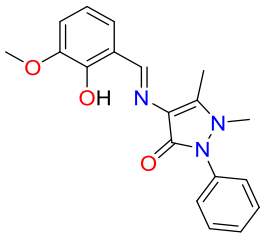

Scheme 1. (E)-4-(2-hydroxy-3-methoxy-benzylideneamino)-2,3-dimethyl-1-phenyl-1,2-dihydropyrazol-5-one (HL1)

The alternating fashion of Co^{II}/Dy^{III} ions in **1**, prompted us to synthesize other Ln analogues of this motif and study their magnetic properties. In addition, the use of anisotropic Co^{II} 3d ion restrains the construction of magnetic coolers,[29] thus an attempt was made to replace these with the more isotropic Ni^{II} ions, which have previously led to Ni^{II}/Gd^{III} CCs with large MCE, i.e. the 48-member metallocycle $Ni_{12}Gd_{36}$[60] and the cage like Ni_6Gd_6.[61] Thus, we herein report a series of five isoskeletal $M^{II}_3Ln^{III}_4$ disk – like CCs formulated as $[Co^{II}_3Gd^{III}_4(\mu_3\text{-}OH)_6(\mathbf{L1})_6(CF_3SO_3)](CF_3SO_3)_5]$ (**2**), $[Co^{II}_3Y^{III}_4(\mu_3\text{-}$

[a] K. Griffiths, C. Harding, Dr. V. N. Dokorou, E. Loukopoulos, S. I. Sampani, Dr. A. Abdul-Sada, Dr. G. E. Kostakis
Department of Chemistry, School of Life Sciences, University of Sussex, Brighton BN1 9QJ, UK, G.Kostakis@sussex.ac.uk, http://www.sussex.ac.uk/lifesci/kostakislab/
[b] Dr. G. J. Tizzard, Prof. S. J. Coles,
UK National Crystallography Service, Chemistry, University of Southampton SO1 71BJ, U.K.
[c] Dr G. Lorusso, Dr. M. Evangelisti
Instituto de Ciencia de Materiales de Aragón(ICMA), CSIC – Universidad de Zaragoza, 50009 Zaragoza, Spain.
[d] Prof. A. Escuer
Department de Quimica Inorganica, i Orgànica, Secció Inorgànica and Institut de Nanociència i Nanotecnologia (IN^2UB), Universitat de Barcelona, Martí Franqués 1-11, 08028 Barcelona, Spain. Albert.escuer@qi.ub.es, http://www.ub.edu/inorgani/recerca/MagMol/magmol.htm
Supporting information for this article is given via a link at the end of the document.

$OH)_6$(**L1**)$_6(CF_3SO_3)](CF_3SO_3)_5]$ (**3**), $[Ni^{II}_3Dy^{III}_4(\mu_3$-$OH)_6$(**L1**)$_6(CF_3SO_3)](CF_3SO_3)_5]$ (**4**), $[Ni^{II}_3Gd^{III}_4(\mu_3$-$OH)_6$(**L1**)$_6(CF_3SO_3)](CF_3SO_3)_5)]$ (**5**), $[Ni^{II}_3Y^{III}_4(\mu_3$-$OH)_6$(**L1**)$_6(CF_3SO_3)](CF_3SO_3)_5]$ (**6**). Synthetic and topological insights as well the magnetic properties of **2**-**6** are discussed, together with an evaluation of the MCE for **5**.

Results and Discussion

Synthetic issues. The previously reported $Co^{II}_3Dy^{III}_4$ CCs **1** was prepared from the room temperature reaction of $Dy(OTf)_3$ and $Co(ClO_4)_2.6H_2O$ with H**L1** in a molar ratio of 2:1:2.5:2.5 (Dy:Co:HL:Et_3N) using MeOH as solvent, yielding crystals after 3 weeks in low yield.[57] When a similar reaction was performed in EtOH, under reflux, an isoskeletal compound formulated $[Co^{II}_3Dy^{III}_4(\mu_3$-$OH)_6$(**L1**)$_6(CF_3SO_3)](ClO_4)_3(CF_3SO_3)_2$ (**1'**) was isolated in only 3 days with moderate yield (Table 1).[57] The latter indicates that the temperature and the solvent of the reaction had a profound effect on the crystallization time and yield of the product. When these two methods were applied to synthesize the Co^{II}/Ln^{III} (Ln= Gd, Y) analogues the yield greatly decreased and when applied to Ni^{II}/Ln^{III} analogues either produced the expected product in very low yield (5%, Table 1, entry 6) or hexagonal shaped crystals were obtained in very low yields after almost 6 weeks (compound **4'**, ESI, Table 1, entry 7). An adaption of the synthetic procedure lead (Table 1, entries 3, 4, 5, 8 and 9) to the formation of expected disk-like CCs with all M^{II}_3/Ln^{III}_4 combinations in very good yields (63-85%), whereas less crystallization time was required. Compounds **2**, **3**, **4**, **5** and **6** were synthesized using the following recipe; EtOH reflux, increased amount of Et_3N and a replacement of $M(ClO_4)_2.6H_2O$ with $M(NO_3)_2.6H_2O$ in a molar ratio 2:1:2.5:12. The change in synthetic protocol resulted in the replacement of counter ion ClO_4 molecules with CF_3SO_3 and caused no change to the central $[M^{II}_3Ln^{III}_4(\mu_3$-$OH)_6L_6(CF_3SO_3)]$ ion.

Crystal Structure Description. Unit cell determinations, IR spectra, elemental analyses and TGA show **2**, **3**, **4**, **5** and **6** to be isoskeletal, therefore only a detailed crystallographic description of **4** will be described here. Crystallographic studies show that **2-4**, crystallize in the orthorhombic space group *Pbca*. The heptanuclear disk like compound, composes of a hexanuclear wheel, three Ni^{II} and three Dy^{III} centers in an alternating fashion, and a central Dy^{III} center. The peripheral six centers form a plane and the central Dy^{III} lies 0.671Å out of it. Six, altering above and below the plane, triply bridging hydroxyl groups support the formation of the disk, whereas a CF_3SO_3 moiety caps the central Dy center ion. The coordination number of the three peripheral and one central Dy^{III} ions is 8 and 7, respectively. The geometry of the central Dy^{III} can be described as a capped octahedron whereas the Dy^{III} ions lying within the wheel is that of a bicapped trigonal prism. The Ni^{II} centers adopt what can be best described as a distorted octahedral geometry. The six ligands coordinate in a similar manner (Scheme S1). All six ligands chelate to a Ni^{II} ion, through the phenoxido oxygen and the imino nitrogen atoms, to a Dy^{III} ion, through the phenoxido and methoxido oxygen atoms, and bond to another Dy^{III} ion through a carbonyl oxygen atom. The angles of the μ_3-OH bridges are within the range 97.2(3) – 106.7(3)°. There are three Dy---Dy distances,3.6470(9) Å, 3.6561(9) Å and 3.6619(12) Å, and nine Ni---Dy distances within the range 3.3715(19) - 3.4806(16) Å. The diameter of the disk is 18.799 Å.

Table 1. Synthetic conditions for reported disc like CCs. Yield % based on Ln^{III}.

Entry	Compound	Synthetic Ratio (Ln:M:HL:Et_3N)	Formula	Solvent	Yield/ %	Crystallisation time/ days
1	**1**	2:1:2.5:2.5	$[Co^{II}_3Dy^{III}_4(\mu_3$-$OH)_6$(**L1**)$_6(CF_3SO_3)](ClO_4)_5$	MeOH	22	21
2	**1'**	2:1:2.5:2.5	$[Co^{II}_3Dy^{III}_4(\mu_3$-$OH)_6$(**L1**)$_6(CF_3SO_3)](ClO_4)_3(CF_3SO_3)_2$	EtOH	45	3
3	**2**	2:1:2.5:12	$[Co^{II}_3Gd^{III}_4(\mu_3$-$OH)_6$(**L1**)$_6(CF_3SO_3)](CF_3SO_3)_5$	EtOH	81	2
4	**3**	2:1:2.5:12	$[Co^{II}_3Y^{III}_4(\mu_3$-$OH)_6$(**L1**)$_6(CF_3SO_3)](CF_3SO_3)_5$	EtOH	77	5
5	**4**	2:1:2.5:12	$[Ni^{II}_3Dy^{III}_4(\mu_3$-$OH)_6$(**L1**)$_6(CF_3SO_3)](CF_3SO_3)_5$	EtOH	69	3
6	**4**	2:1:2.5:2.5	$[Ni^{II}_3Dy^{III}_4(\mu_3$-$OH)_6$(**L1**)$_6(H_2O)](ClO_4)_6$	EtOH	5	25
7	**4'**	2:1:2.5:2.5	$[Ni^{II}_3Dy^{III}_4(\mu_3$-$OH)_6$(**L1**)$_6(H_2O)](ClO_4)_6$	MeOH	12	38
8	**5**	2:1:2.5:12	$[Ni^{II}_3Gd^{III}_4(\mu_3$-$OH)_6$(**L1**)$_6(CF_3SO_3)](CF_3SO_3)_5)$	EtOH	71	2
9	**6**	2:1:2.5:12	$[Ni^{II}_3Y^{III}_4(\mu_3$-$OH)_6$(**L1**)$_6(CF_3SO_3)](CF_3SO_3)_5$	EtOH	68	7

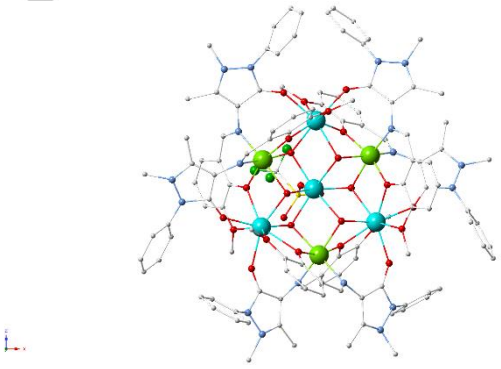

Figure 1. Molecular structure of **4**. Color code; green: Ni^{II}; light blue: Dy^{III}; yellow: carbon; pale blue: nitrogen; red: oxygen; yellow: Sulphur; fluorine: light green.

ESI-MS Studies. To further confirm the identity of the reported compounds, we performed a broad electrospray ionization mass spectrometry for compounds **2**, **3**, **4**, **5** and **6**. We observed three main regions for the analogues showing three distinct fragments in each region, perfectly corresponding to the tetracationic, tricationic and dicationic fragments respectively; $[M_3Ln_4(\mu_3$-$OH)_6(C_{19}H_{18}N_3O_3)_6(CF_3SO_3)]^{4+}$, $[M_3Ln_4(\mu_3$-$OH)_6(C_{19}H_{18}N_3O_3)_6(CF_3SO_3)_3]^{3+}$ and $[M_3Ln_4(\mu_3$-

$OH)_6(C_{19}H_{18}N_3O_3)_6(CF_3SO_3)_4]^{2+}$ (Fis S1-S5). Conversely the **6** analogue only demonstrates the $[Ni_3Y_4(\mu_3\text{-}OH)_6(C_{19}H_{18}N_3O_3)_6(CF_3SO_3)_4]^{2+}$ fragment (Fig S3). Values assigned to these fragments corresponding to CC are shown in Table 2. Each of these fragments corresponds to the $[M_3Ln_4(\mu_3\text{-}OH)_6(L_6)]$ core with additional OTf counter ions.

Table 2. m/z fragment vales for reported $M^{II}_3Ln^{III}_4$ CC.

Compound	$[M_3Ln_4(\mu_3\text{-}OH)_6(C_{19}H_{18}N_3O_3)_6(CF_3SO_3)_4]^{2+}$ /m/z	$[M_3Ln_4(\mu_3\text{-}OH)_6(C_{19}H_{18}N_3O_3)_6(CF_3SO_3)_3]^{3+}$ /m/z	$[M_3Ln_4(\mu_3\text{-}OH)_6(C_{19}H_{18}N_3O_3)_6(CF_3SO_3)]^{4+}$ /m/z
2	1762.06	1125.39	807.06
3	1624.03	1038.02	761.19
4	1771.14	1132.07	774.82
5	1760.61	1124.41	768.09
6	1624.09	N/A	N/A

Thermogravimetric analysis. TGA measurements were performed to examine the thermal stability of selected compounds. In the cases of **2** and **6** (Figs S6 – S7, ESI), the first mass loss corresponds to the loss of the counter-anions. The stability of the remaining core is then retained up to the region of ~300 °C, where gradual decomposition takes place. The final residue fits well to the analogous oxide $[Co_3Gd_4O_9$ for **2** calculated (24.86%) found (24.14%) and $Ni_3Y_4O_9$ for **6** calculated (19.05%) found (19.43%)].

Topological features. There are few examples of 3d/4f disk-like CCs reported in the literature. The first reported examples demonstrating the disk-like or **3,6M7-1**[62] topology were the Mn^{IV}_6Ce disks reported by Christou et al.[63,64] These were followed by $Cu^{II}_6Pr^{III}$,[65] $Mn^{II}_3Ln^{III}_4$,[66] $Cu^{II}_5Ln^{III}_2$,[67] $Co^{II}_3Dy^{III}_4$,[57] and $Co^{II}_2Dy^{III}_5$[59] examples (Table 3). The seven previous reported examples of 3d/4f **3,6M7-1** CCs are shown (Table 3 entries 1-7) and to the best of our knowledge (**4-6**) are the first examples of Ni^{II}/Ln^{III} CCs of this topology. Whereas **3** and **2** are the first examples of Co^{II}/Y^{III} and Co^{II}/ Gd^{III} discs respectively, whilst both are also the fourth and fifth examples of Co^{II}/Ln^{III} disks. There are three configurations for the 3d and 4f cation nodes within the disk, dependent on the 3d and 4f ratio. The first (3/4, A Figure 2) incorporates the presence of an Ln node in the center of the disk. This configuration is found in all $M^{II}_3Ln^{III}_4$ (Table 3 entries 1, 6, 7 and 8) and all form $[Mn^{II}_3Ln^{III}_4(\mu_3\text{-}O)_6]$ cores. The next (5/2 or 2/5 B Figure 2) configuration involves $Cu^{II}_5Ln^{II}_2$ and $Co^{II}_2Dy^{III}_5$ (Table 3 Entries 2 and 7). The Ln or the Co nodes can be found in the periphery sandwiched between two 3d nodes each side, with a central Cu or Dy node, respectively. The last (6/1, C Figure 2) configuration is seen in $Mn^{IV}_6Ce^{IV}$ and Cu^{II}_6Pr CCs; the 3d ions form the periphery and the 4f ion occupies the central node. With this report, Schiff Base ligands (H**L1** and H_3**L3**) have been the most successful in synthesizing 3d/4f **3,6M7-1** CCs, however these are limited to the M^{II}/Ln^{III} valences. Whereas ligands containing carboxylic acid groups have been used to form unique Mn^{IV}/Ln^{IV} clusters as well as the M^{II}/Ln^{III} valences. Though it is evident there are distinct types of **3,6M7-1** CCs it is difficult to relate these to the types of ligand with the limited number of examples. None of the previously reported examples have been investigated for the magnitude of their MCE, whereas $Co^{II}_3Dy^{III}_4$, $Cu^{II}_5Dy^{III}_2$, $Cu^{II}_5Ho^{III}_2$ were found to have SMM properties at low energy barriers.

Table 3. Reported 3d/4f CCs with **3,6M7-1** topology.

Entry	Formula	Metals	Ligand	Ref
1	$[Mn^{II}_3Ln^{III}_4(Piv)_{12}$(**L2**)$_2(H2O)_3]\cdot H_2O$ Ln= La, Pr, Nd, Gd	Mn^{II}/Ln^{II}	H_3**L2**	[66]
2	$[Cu^{II}_5Ln^{III}_2$(**L3**)$_2(\mu_3\text{-}OH)_4(\mu\text{-}OH_2)_2(\mu\text{-}OAc)_2(OAc)_2(OH_2)_2](NO_3)_2(H_2O)_2$ Ln=Y, Lu, Dy, Ho, Er, Yb	Cu^{II}/Ln^{II}	H_3**L3**	[67]
3	$[Mn^{IV}Ce^{IV}_6O_9$(**L4**)$_9(H_2O)_2(MeOH)](ClO_4)$	Mn^{IV}/Ce^{IV}	H**L4**	[63]
4	$[Mn_6CeO_9(O_2CR)_9(X)(H_2O)_2]^{y+}$ (R = Me (**L4**), X = NO_3^-, y = 0 (**2**); R = Me (**L5**), X = MeOH, y = +1 (**3**); R = Et, X = NO_3^-, y = 0	Mn^{IV}/Ce^{IV}	H**L4**, H**L5**	[64]
5	$[Cu^{II}_6Pr^{III}$(**L6**)$_6][Pr^{III}(H_2O)_{10}].14H_2O$	Cu^{II}/Pr^{III}	H_3**L6**	[65]
6	$[Co^{II}_3Dy^{III}_4(\mu_3\text{-}OH)_6$(**L1**)$_6(CF_3SO_3)](ClO_4)_5$	Co^{II}/Ln^{II}	H**L1**	[57]
7	$[Co^{II}_2Dy^{III}_5(\mu_3\text{-}OH)_6$(**L1**)$_2(Piv)_8(NO_3)_4]\cdot 4CH_3CN$	Co^{II}/Ln^{II}	**HL1**	[59]
8	$[Co^{II}_3Ln^{III}_4(\mu_3\text{-}OH)_6$(**L1**)$_6(CF_3SO_3)](CF_3SO_3)_5$ Ln= Gd, Y	Co^{II}/Ln^{II}	H**L1**	This Work
9	$[Ni^{II}_3Ln^{III}_4(\mu_3\text{-}OH)_6$(**L1**)$_6(CF_3SO_3)](CF_3SO_3)_5$ Ln=Dy, Gd, Y	Ni^{II}/Ln^{III}	H**L1**	This Work

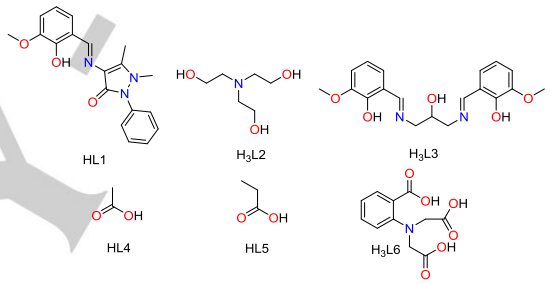

Scheme 2. Ligands used in the synthesis of 3d/4f **3,6M7-1** CCs

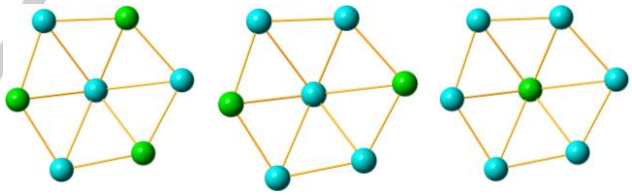

Figure 2. Configurations (**A**, **B** and **C**) of 3d/4f nodes for reported **3,6M7-1** CCs. Green and light blue nodes correspond to 3d and 4f ions, respectively.

Magnetic Properties. Susceptibility measurements were performed for **2**, **4** and **5** and for the Ni-Y complex **6** in order to check the degree of interaction between the d cations, Figure 2. The $\chi_M T$ value for **2** at room temperature is 42.87 $cm^3\cdot mol^{-1}\cdot K$, larger than the corresponding spin-only value for three Co^{II} and four Gd^{III} isolated cations of 37.125 $cm^3\cdot mol^{-1}\cdot K$. On cooling the $\chi_M T$ value decreases very slightly in the 300-40 K and below this temperature increases continuously up to 60.23 $\chi_M T$ $cm^3\cdot mol^{-1}\cdot K$ at 2 K. Compound **4** shows a room temperature $\chi_M T$ value of 61.43 $cm^3\cdot mol^{-1}\cdot K$ that decreases to a minimum value of 57.21 $cm^3\cdot mol^{-1}\cdot K$ at 15 K, increasing at lower temperatures up to 98.5 $cm^3\cdot mol^{-1}\cdot K$ at 2 K. The initial decrease should be attributed to the depopulation of the Stark levels of the Dy^{III} cation. Compound **5** shows a $\chi_M T$ value of 36.09 $cm^3\cdot mol^{-1}\cdot K$ at 300 K, somewhat

larger than the 34.50 $cm^3 \cdot mol^{-1} \cdot K$ value expected for three Ni^{II} and four Gd^{III} non-interacting cations per molecule, thus suggesting that correlations are sizeable at room temperature. On cooling, the $\chi_M T$ product increases slightly in the 300-50 K range and fast below 50 K, reaching the maximum value of 76.2 $cm^3 \cdot mol^{-1} \cdot K$ at 2.6 K, below which it decays to 75.0 $cm^3 \cdot mol^{-1} \cdot K$ at 2 K, likely because of weak antiferromagnetic interactions or crystal-field effects. The shape and low-temperature $\chi_M T$ values clearly indicate that the dominant interactions are ferromagnetic for the three complexes. Magnetization experiments (Fig. 3 right) show a fast increase at low fields and a further slow increase of the magnetization, reaching quasi saturated values of 28.1 $N\mu_B$ for **4**, 35.7 $N\mu_B$ for **2** and 34.9 $N\mu_B$ for **5,** coherent with the maximum ferromagnetic *S* ground states for **2** and **5** (*S* = 18.5 and 17 respectively). Fit of the experimental data was not possible for the anisotropic Co_3Gd_4 and Ni_3Dy_4 complexes **2** and **4**, but a spin-only attempt was performed for the Ni_3Gd_4 complex **5**. We have also measured the response of the Ni_3Y_4 complex **6**, that shows a constant $\chi_M T$ value of 3.5 $cm^3 \cdot mol^{-1} \cdot K$ between 300-6 K and a decay below this temperature down to a final value of 2.80 $cm^3 \cdot mol^{-1} \cdot K$ at 2 K. This measure indicates that there is no interaction between the Ni^{II} cations and that complex **6** magnetically behaves as three isolated Ni^{II} cations with a *g* value of 2.16. Next, simultaneous fits of $\chi_M T$ and $M(H, T)$ data (Fig. 4) were carried out for **5** by using PHI program[68], assuming that only the Ni-Gd and the Gd-Gd pathways are operative and that g_{Ni} = 2.16. The best fit, solid lines in Figs. 3 and 4, gives: J_1(Gd-Gd) = −0.17 cm^{-1} and J_2(Ni-Gd) = 0.62 cm^{-1}. It is noteworthy to mention that similar fitting curves of $\chi_M T$ and $M(H, T)$ can also be obtained by constraining J_1(Gd-Gd) and J_2(Ni-Gd) to be both ferromagnetic and by adding a weak antiferromagnetic effective *zJ* interaction to take into account intermolecular couplings. However, we should safely disregard this second set of parameters because, contrary to the first one, it cannot be used to reproduce satisfactorily the heat capacity results that we report below.

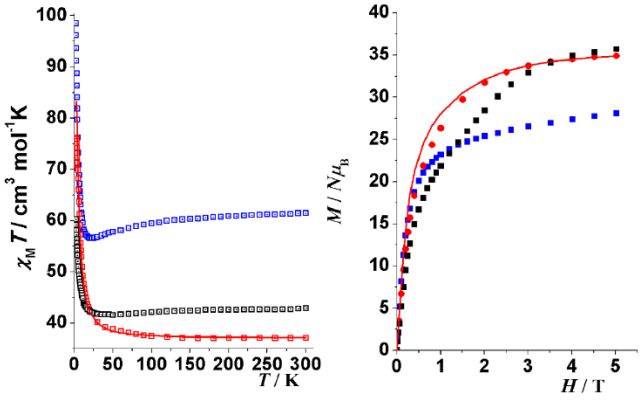

Figure 3. Left $\chi_M T$ product for **2** (black), **4** (blue) and **5** (red), for applied field 0.1 T. Solid line shows the fit of the experimental data for **5**. Right, magnetization plots for **2** (black), **4** (blue) and **5** (red).

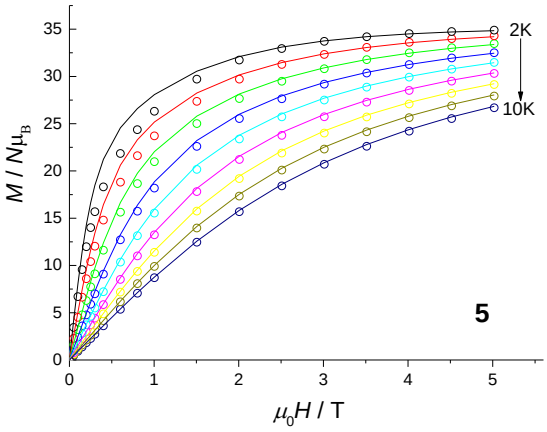

Figure 4. Isothermal magnetization curves for T = 2−10 K, step 1 K. Solid lines are the best fit curves obtained by using spin-only model and by fixing g_{Ni} = 2.16; the coupling constant found from the fitting are J_1(Gd-Gd) = -0.17 cm^{-1} and J_2(Ni-Gd) = 0.62 cm^{-1}.

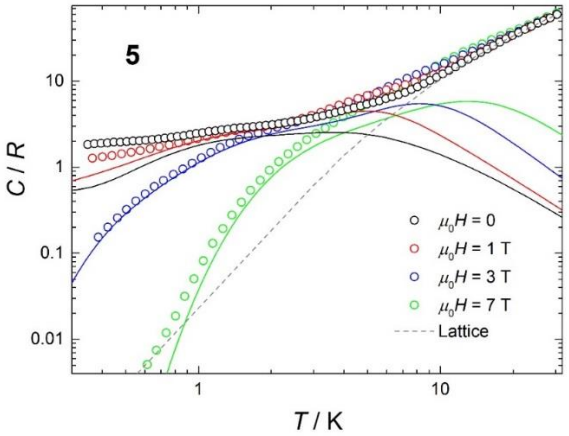

Figure 5. Temperature-dependence of the molar heat capacity, normalized to the gas constant *R*, for **5**, collected for the labelled applied fields. Solid lines are the calculated magnetic contributions for J_1(Gd-Gd) = -0.17 cm^{-1} and J_2(Ni-Gd) = 0.62 cm^{-1}, while dashed line is the non-magnetic lattice contribution.

Heat Capacity. Figure 5 shows the experimental molar heat capacity *C* for compound **5**, collected for the temperature range 0.35-30 K and for several applied magnetic fields. The heat capacity is best understood by comparing the experimental data with the calculated curves (solid lines) on the basis of the spin-only model and parameters J_1(Gd-Gd) = -0.17 cm^{-1} and J_2(Ni-Gd) = 0.62 cm^{-1}, obtained from fitting the susceptibility and magnetization data. Overall, the agreement is significantly good, with the main discrepancy gradually taking place on increasing *T* above 10-15 K. This discrepancy is due to a non-magnetic contribution that we ascribe to lattice vibrations and can be described by the Debye model (dotted line), which simplifies to a $C/R = aT^3$ dependence at the lowest temperatures, where a = 2.3 x10^{-2} K^{-3}. The magnetic contribution to the heat capacity is

strongly dependent on the applied field, especially for fields larger than 1 T. At the lowest temperatures, the calculated curves deviate from the experimental ones for zero field and less so for $\mu_0 H$ = 1 T. This is very likely due to weak, though sizeable, magnetic interactions acting between the molecules, probably of dipolar origin, which are not included in our calculations.

Magnetocaloric Effect. Finally, we evaluate the MCE for Ni_3Gd_4, namely, we determine its magnetic entropy change, ΔS_m, and adiabatic temperature change ΔT_{ad} for selected values of the applied field change $\Delta H = H$ - 0. Note that ΔS_m can be calculated from the heat capacity and magnetization data by using the relations:

$$\Delta S_m(T, \Delta H) = S_m(T, H) - S_m(T, 0) = \int_0^T \frac{C_m(T,H)}{T} dT - \int_0^T \frac{C_m(T,0)}{T} dT, \quad (1)$$

$$\Delta S_m(T, \Delta H) = \int_0^H \left(\frac{\partial M(T,H)}{\partial T}\right)_H dH, \quad (2)$$

where S_m is the magnetic entropy and C_m is the magnetic heat capacity, which we obtain by subtracting the lattice contribution (dashed line in Figure 5) to the total heat capacity C. The adiabatic temperature change can then be obtained straigthforwardly as temperature changes from the entropic data.

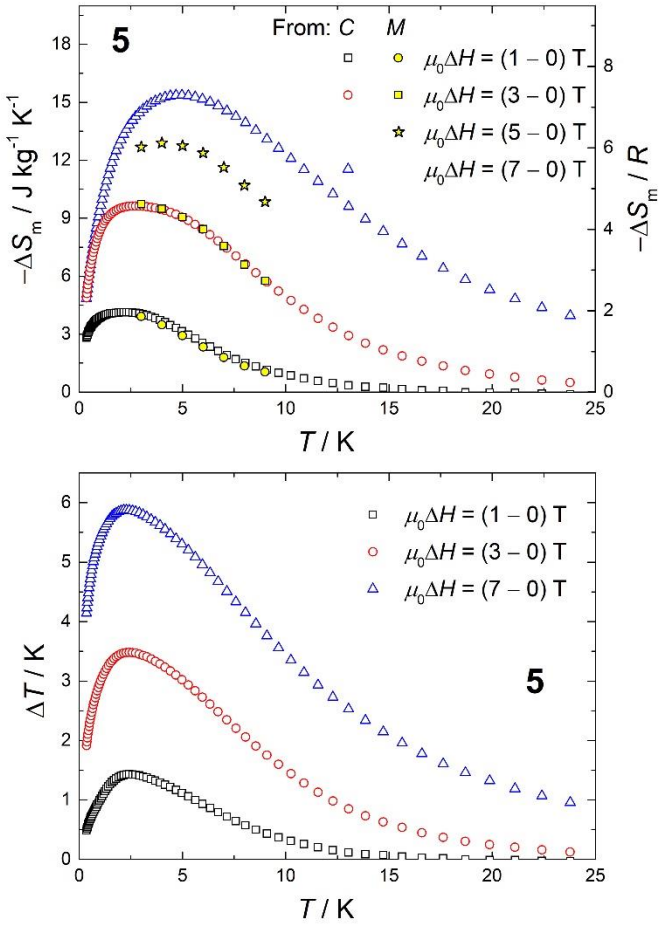

Figure 6. (Top) Magnetic entropy change *vs T*, for several values of the applied field change ΔH, as labelled. These data are calculated by making use of the magnetization and heat capacity data. Vertical axis reports units in $Jkg^{-1}K^{-1}$ (left) and molar R (right). (Bottom) Adiabatic temperature change *vs T* for the labelled applied field change, as obtained from heat capacity data.

The results are shown in Figure 6, where one can notice that the two sets of data for ΔS_m that we obtain from $C(T,H)$ and $M(T,H)$ are consistent to each other, thus confirming that the procedures used are correct. For $\mu_0\Delta H$ = 7 T, $-\Delta S_m$ reaches 7.3 R = 15.4 $Jkg^{-1}K^{-1}$ at T = 5.0 K, while ΔT_{ad} = 5.9 K at T = 2.3 K. Magnetic correlations inhibit the system to reach the whole available magnetic entropy that for four Gd^{III} and three Ni^{II} ions per molecule amounts to $4R\ln(2s_{Gd}+1) + 3R\ln(2s_{Ni}+1) = 11.62\ R$, where S_{Gd} = 7/2 and S_{Ni} = 1. The values of ΔS_m for **5**, when expressed per molar R, are similar to the corresponding ones reported for other Ni-Gd compounds,[46,69,70] whereas they compare less favourably when expressed per unit mass, because the metal/non-metal ratio is relatively modest in **5**.

Conclusions

Altering the synthetic procedure of the previously reported heptanuclear disk like CC **1**, a family of isoskeletal compounds formulated $[M^{II}_3Ln^{III}_4(\mu_3\text{-}OH)_6(\mathbf{L1})_6(CF_3SO_3)](CF_3SO_3)_5]$ is obtained in higher yields and shorter crystallization times. To the best of our knowledge compounds **4** – **6** represent the first examples of Ni^{II}/Ln^{III} CCs derived from this ligand and bearing this disk-like topology. Moreover, **2** and **3** are the first disk-like examples in Co^{II}/ Gd^{III} and Co^{II}/Y^{III} cluster chemistry, respectively. All reported compounds are solution stable and demonstrate three characteristic regions of peaks when analyzed with ESI-MS. The study of their magnetic properties revealed a dominant ferromagnetic coupling, while compound **5** shows magnetocaloric properties at liquid-helium temperatures. The present work illustrates the effectiveness of the proposed synthetic strategy to synthesize polynuclear CCs with fascinating magnetic properties. Ongoing investigations for the synthesis of other polynuclear compounds using this ligand are in progress.

Experimental Section

Materials. Chemicals (reagent grade) were purchased from Sigma Aldrich and Alfa Aesar. All experiments were performed under aerobic conditions using materials and solvents as received. *Safety note*: Perchlorate salts are potentially explosive; such compounds should be used in small quantities and handled with caution and utmost care at all times.

Instrumentation. IR spectra were recorded over the range of 4000-650 cm^{-1} on a Perkin Elmer Spectrum One FT-IR spectrometer fitted with a UATR polarization accessory. ESI-MS date were obtained on Bruker Daltonics Fourier transform ion cyclotron (FTICR-MS) while the EI (at 70 eV) were obtained using Fissions instrument VG Autospec. TGA analysis was performed on a TA Instruments Q-50 model (TA, Surrey, UK) under nitrogen and at a scan rate of 10 °C/min (University of Sussex).

Magnetic studies. Variable-temperature and variable-field magnetic studies were performed using a MPMS-5 Quantum Design magnetometer operating at 0.03 T in the 300-2.0 K range and with applied fields up to 5T. Diamagnetic corrections were applied to the observed paramagnetic

susceptibility using Pascal's constants. Heat capacity measurements were carried out by using a Quantum Design PPMS system, equipped with a ^{3}He cryostat. The experiments were performed on a thin pressed pellet (ca. 1 mg) of a polycrystalline sample, thermalized by ca. 0.2 mg of Apiezon N grease, whose contribution was subtracted by using a phenomenological expression.

Ligand synthesis. The synthesis of H**L1** was performed following the reported procedure.[36]

Preparation of compounds 2 – 6. $Ln(OTf)_3$ (0.2mmol), $Co(NO_3)_2.6H_2O$ (0.1mmol, 58mg), H**L1** (0.2mmol, 34mg) and Et_3N (1.2mmol, 26.8µL) were refluxed for 2h in EtOH (20mL). The reaction mixture was subsequently cooled and filtered. The filtrate was left for slow evaporation between 4-8 days before red crystals suitable for Single X-Ray were collected. These were dried overnight. CHN (**2**) $[Co^{II}_3Gd^{III}_4(\mu_3\text{-}OH)_6(\mathbf{L1})_6(CF_3SO_3)](CF_3SO_3)_5]$(expected) C-37.68%, H-3.01%, N-6.60% (observed) C-37.59%, H.3.04%, N-6.71%; A similar procedure was followed for the synthesis of **3** – **6** using the corresponding metal salts. CHN (**3**) $[Co^{II}_3Y^{III}_4(\mu_3\text{-}OH)_6(\mathbf{L1})_6(CF_3SO_3)](CF_3SO_3)_5]$ (expected) C-40.62%, H-3.24%, N-7.11% (observed) C-40.71%, H-3.33%, N-7.21%. CHN (**4**); $[Ni^{II}_3Gd^{III}_4(\mu_3\text{-}OH)_6L_6(CF_3SO_3)](CF_3SO_3)_5)$ (expected) C-37.71%, H-3.01%, N-6.60% (observed)C-37.82%, H.2.98%, N-6.55%; CHN (**5**) $[Ni^{II}_3Dy^{III}_4(\mu_3\text{-}OH)_6(\mathbf{L1})_6(CF_3SO_3)](CF_3SO_3)_5]$ (expected) C-37.47%, H-2.99%, N-6.56% (observed) C-37.50%, H-3.09%, N-6.46% ;CHN (**6**) $[Ni^{II}_3Y^{III}_4(\mu_3\text{-}OH)_6(\mathbf{L1})_6(CF_3SO_3)](CF_3SO_3)_5]$ (expected) C-40.66%, H-3.24%, N-7.12% (observed) C-40.59%, H-3.23%, N-7.15%;

X-ray Crystallography. Unit cells (Table S1) for **2**, **5** and **6** (ω- scans) were obtained at the University of Sussex by use of an Agilent Xcalibur Eos Gemini Ultra diffractometer with CCD plate detector under a flow of nitrogen gas at 293(2) K for **2** or 173(2) K for **5** and **6** using Mo Kα radiation (λ = 0.71073 Å). Data for **3, 4** and **4'** were collected at the National Crystallography Service, University of Southampton[71] on a Rigaku FRE+ diffractometer equipped with a HG Saturn 724+ CCD detector under a flow of nitrogen gas at 100(2) K, processed with CrysAlisPro and solved by intrinsic phasing methods with SHELXT.[72] All crystal structures were then refined on Fo2 by full-matrix least-squares refinements using SHELXL.[72] All non-H atoms were refined with anisotropic thermal parameters, and H-atoms were introduced at calculated positions and allowed to ride on their carrier atoms. Geometric/crystallographic calculations were performed using PLATON,[73] Olex2,[74] and WINGX[75] packages; graphics were prepared with Crystal Maker.[76] Crystallographic details are given in Table S1. CCDC 1545359 - 1545361.

Acknowledgements

We thank the EPSRC UK National Crystallography Service at the University of Southampton[71] for the collection of the crystallographic data for compounds **3**, **4** and **4'**, the RDF (V. N. D.) and JRA summer fellowship (C. H.) from the University of Sussex. A. E., G. L. and M. E. thank the Ministerio de Economía, Industria y Competitividad for financial support (Projects CTQ2015-63614-P and MAT2015-68204-R) and for a postdoctoral contract (to G. L.).

Keywords: coordination clusters • magnetic properties • topology • Schiff Base • disk-like

[1] J.-B. Peng, X.-J. Kong, Q.-C. Zhang, M. Orendáč, J. Prokleška, Y.-P. Ren, L.-S. Long, Z. Zheng, L.-S. Zheng, *J. Am. Chem. Soc.* **2014**, *136*, 17938–17941.

[2] C. Papatriantafyllopoulou, E. E. Moushi, G. Christou, A. J. Tasiopoulos, *Chem. Soc. Rev.* **2016**, *45*, 1597–1628.

[3] W.-P. Chen, P.-Q. Liao, Y. Yu, Z. Zheng, X.-M. Chen, Y.-Z. Zheng, *Angew. Chem. Int. Ed.* **2016**, *55*, 9375–9379.

[4] G. E. Kostakis, in *Elsevier Ref. Modul. Chem. Mol. Sci. Chem. Eng.* (Ed.: J. Reedijk), Elsevier, Waltham, MA, **2016**, pp. 1–53.

[5] J. Long, J. Rouquette, J.-M. Thibaud, R. A. S. Ferreira, L. D. Carlos, B. Donnadieu, V. Vieru, L. F. Chibotaru, L. Konczewicz, J. Haines, et al., *Angew. Chem. Int. Ed.* **2015**, *54*, 2236–2240.

[6] J. Jankolovits, C. M. Andolina, J. W. Kampf, K. N. Raymond, V. L. Pecoraro, *Angew. Chem. Int. Ed.* **2011**, *50*, 9660–9664.

[7] F. Evangelisti, R. Moré, F. Hodel, S. Luber, G. R. Patzke, *J. Am. Chem. Soc.* **2015**, *137*, 11076–11084.

[8] P. Buchwalter, J. Rosé, P. Braunstein, *Chem. Rev.* **2015**, *115*, 28–126.

[9] K. Griffiths, P. Kumar, G. R. Akien, N. F. Chilton, A. Abdul-Sada, G. J. Tizzard, S. J. Coles, G. E. Kostakis, *Chem. Commun.* **2016**, *52*, 7866–7869.

[10] R. G. Pearson, *J. Chem. Educ.* **1968**, *45*, 581.

[11] R. E. P. Winpenny, *J. Chem. Soc. Dalt. Trans.* **2002**, 1–10.

[12] J. Ferrando-Soria, A. Fernandez, E. Moreno Pineda, S. A. Varey, R. W. Adams, I. J. Vitorica-Yrezabal, F. Tuna, G. A. Timco, C. A. Muryn, R. E. P. Winpenny, *J. Am. Chem. Soc.* **2015**, *137*, 7644–7647.

[13] J. Wu, L. Zhao, L. Zhang, X.-L. Li, M. Guo, A. K. Powell, J. Tang, *Angew. Chemie Int. Ed.* **2016**, *55*, 15574–15578.

[14] Y.-K. Deng, H.-F. Su, J.-H. Xu, W.-G. Wang, M. Kurmoo, S.-C. Lin, Y.-Z. Tan, J. Jia, D. Sun, L.-S. Zheng, *J. Am. Chem. Soc.* **2016**, *138*, 1328–1334.

[15] T. Pugh, N. F. Chilton, R. A. Layfield, *Angew. Chemie Int. Ed.* **2016**, *55*, 11082–11085.

[16] Y.-S. Ding, N. F. Chilton, R. E. P. Winpenny, Y.-Z. Zheng, *Angew. Chemie Int. Ed.* **2016**, *55*, 16071–16074.

[17] J. J.-L. Liu, Y.-C. Chen, J. J.-L. Liu, V. Vieru, L. Ungur, J.-H. Jia, L. F. Chibotaru, Y. Lan, W. Wernsdorfer, S. Gao, et al., *J. Am. Chem. Soc.* **2016**, *138*, 5441–50.

[18] Y.-C. Chen, J.-L. Liu, L. Ungur, J. Liu, Q.-W. Li, L.-F. Wang, Z.-P. Ni, L. F. Chibotaru, X.-M. Chen, M.-L. Tong, *J. Am. Chem. Soc.* **2016**, *138*, 2829–2837.

[19] A. M. Ako, I. J. Hewitt, V. Mereacre, R. Clérac, W. Wernsdorfer, C. E. Anson, A. K. Powell, *Angew. Chemie Int. Ed.* **2006**, *45*, 4926–4929.

[20] M. Manoli, S. Alexandrou, L. Pham, G. Lorusso, W. Wernsdorfer, M. Evangelisti, G. Christou, A. J. Tasiopoulos, *Angew. Chem. Int. Ed.* **2016**, *55*, 679–684.

[21] A. M. Ako, V. Mereacre, R. Clérac, W. Wernsdorfer, I. J. Hewitt, C. E. Anson, A. K. Powell, *Chem. Commun.* **2009**, 544–546.

[22] T. C. Stamatatos, K. A. Abboud, W. Wernsdorfer, G. Christou, *Angew. Chem. Int. Ed.* **2007**, *46*, 884–888.

[23] R. Modak, Y. Sikdar, G. Cosquer, S. Chatterjee, M. Yamashita, S. Goswami, *Inorg. Chem.* **2016**, *55*, 691–699.

[24] X.-Q. Song, P.-P. Liu, Y.-A. Liu, J.-J. Zhou, X.-L. Wang, *Dalton Trans.* **2016**, *45*, 8154–8163.

[25] L. Zhao, J. Wu, H. Ke, J. Tang, *Inorg. Chem.* **2014**, *53*, 3519–3525.

[26] J. W. Sharples, D. Collison, *Coord. Chem. Rev.* **2014**, *260*, 1–20.

[27] L. Li, Y. Zhang, M. Avdeev, L. F. Lindoy, D. G. Harman, R. Zheng, Z. Cheng, J. R. Aldrich-Wright, F. Li, *Dalton Trans.* **2016**, *45*, 9407–9411.

[28] C. D. Polyzou, A. Baniodeh, N. Magnani, V. Mereacre, N. Zill, C. E. Anson, S. P. Perlepes, A. K. Powell, *RSC Adv.* **2015**, *5*, 10763–10767.

[29] J. A. Sheikh, A. Clearfield, *Inorg. Chem.* **2016**, *55*, 8254–8256.

[30] J.-L. Liu, W.-Q. Lin, Y.-C. Chen, S. Gómez-Coca, D. Aravena, E. Ruiz, J.-D. Leng, M.-L. Tong, *Chem. Eur. J.* **2013**, *19*, 17567–17577.

[31] J. W. Sharples, Y. Zheng, F. Tuna, E. J. L. McInnes, D. Collison, *Chem. Commun.* **2011**, *47*, 7650–7652.

[32] G. Guthausen, J. R. Machado, B. Luy, A. Baniodeh, A. K. Powell, S. Krämer, F. Ranzinger, M. P. Herrling, S. Lackner, H. Horn, *Dalton Trans.* **2015**, *44*, 5032–5040.

[33] Y.-Z. Zheng, M. Evangelisti, F. Tuna, R. E. P. Winpenny, *J. Am. Chem. Soc.* **2012**, *134*, 1057–1065.

[34] R. Sessoli, A. K. Powell, *Coord. Chem. Rev.* **2009**, *253*, 2328–2341.

[35] E. C. Sañudo, L. Rosado Piquer, *Dalton Trans.* **2015**, *44*, 8771–8780.
[36] K. Liu, W. Shi, P. Cheng, *Coord. Chem. Rev.* **2015**, *289–290*, 74–122.
[37] J.-L. Liu, J.-Y. Wu, Y.-C. Chen, V. Mereacre, A. K. Powell, L. Ungur, L. F. Chibotaru, X.-M. Chen, M.-L. Tong, *Angew. Chemie Int. Ed.* **2014**, *53*, 12966–12970.
[38] K. C. Mondal, A. Sundt, Y. Lan, G. E. Kostakis, O. Waldmann, L. Ungur, L. F. Chibotaru, C. E. Anson, A. K. Powell, *Angew. Chem. Int. Ed.* **2012**, *51*, 7550–7554.
[39] X.-L. Li, F.-Y. Min, C. Wang, S.-Y. Lin, Z. Liu, J. Tang, *Dalt. Trans.* **2015**, *44*, 3430–3438.
[40] J. Goura, R. Guillaume, E. Rivière, V. Chandrasekhar, *Inorg. Chem.* **2014**, *53*, 7815–7823.
[41] S. K. Langley, D. P. Wielechowski, B. Moubaraki, K. S. Murray, *Chem. Commun.* **2016**, *52*, 10976–10979.
[42] I. A. Kühne, N. Magnani, V. Mereacre, W. Wernsdorfer, C. E. Anson, A. K. Powell, *Chem. Commun.* **2014**, *50*, 1882–1885.
[43] Y.-Z. Zheng, G.-J. Zhou, Z. Zheng, R. E. P. Winpenny, *Chem. Soc. Rev.* **2014**, *43*, 1462–75.
[44] G. Karotsis, M. Evangelisti, S. Dalgarno, E. Brechin, *Angew. Chem. Int. Ed.* **2009**, *48*, 9928–9931.
[45] G. Karotsis, S. Kennedy, S. J. Teat, C. M. Beavers, D. A. Fowler, J. J. Morales, M. Evangelisti, S. J. Dalgarno, E. K. Brechin, *J. Am. Chem. Soc.* **2010**, *132*, 12983–12990.
[46] T. N. Hooper, J. Schnack, S. Piligkos, M. Evangelisti, E. K. Brechin, *Angew. Chem. Int. Ed.* **2012**, *51*, 4633–4636.
[47] J.-D. Leng, J.-L. Liu, M.-L. Tong, *Chem. Commun.* **2012**, *48*, 5286–5288.
[48] S. K. Langley, N. F. Chilton, B. Moubaraki, T. Hooper, E. K. Brechin, M. Evangelisti, K. S. Murray, *Chem. Sci.* **2011**, *2*, 1166–1169.
[49] A. Chakraborty, P. Bag, J. Goura, A. K. Bar, J. P. Sutter, V. Chandrasekhar, *Cryst. Growth Des.* **2015**, *15*, 848–857.
[50] J. Goura, V. Mereacre, G. Novitchi, A. K. Powell, V. Chandrasekhar, *Eur. J. Inorg. Chem.* **2015**, *2015*, 156–165.
[51] M. Andruh, *Dalton Trans.* **2015**, *44*, 16633–16653.
[52] J. Wu, L. Zhao, M. Guo, J. Tang, *Chem. Commun.* **2015**, *51*, 17317–17320.
[53] E. C. Mazarakioti, K. M. Poole, L. Cunha-Silva, G. Christou, T. C. Stamatatos, *Dalton Trans.* **2014**, *43*, 11456–11460.
[54] L.-F. Zou, L. Zhao, Y.-N. Guo, G.-M. Yu, Y. Guo, J. Tang, Y.-H. Li, *Chem. Commun.* **2011**, *47*, 8659–8661.
[55] L. Zhang, L. Zhao, P. Zhang, C. Wang, S.-W. Yuan, J. Tang, *Inorg. Chem.* **2015**, *54*, 11535–11541.
[56] J. Wu, L. Zhao, L. Zhang, X. L. Li, M. Guo, J. Tang, *Inorg. Chem.* **2016**, *55*, 5514–5519.
[57] E. Loukopoulos, B. Berkoff, A. Abdul-Sada, G. J. Tizzard, S. J. Coles, A. Escuer, G. E. Kostakis, *Eur. J. Inorg. Chem.* **2015**, *2015*, 2646–2649.
[58] E. Loukopoulos, B. Berkoff, K. Griffiths, V. Keeble, V. N. Dokorou, A. C. Tsipis, A. Escuer, G. E. Kostakis, *CrystEngComm* **2015**, *17*, 6753–6764.
[59] B. Berkoff, K. Griffiths, A. Abdul-Sada, G. J. Tizzard, S. J. Coles, A. Escuer, G. E. Kostakis, *Dalton Trans.* **2015**, *44*, 12788–12795.
[60] J.-B. Peng, Q.-C. Zhang, X.-J. Kong, Y.-P. Ren, L.-S. Long, R.-B. Huang, L.-S. Zheng, Z. Zheng, *Angew. Chem. Int. Ed.* **2011**, *50*, 10649–10652.
[61] Y. Z. Zheng, M. Evangelisti, R. E. P. Winpenny, *Angew. Chemie - Int. Ed.* **2011**, *50*, 3692–3695.
[62] G. E. Kostakis, V. A. Blatov, D. M. Proserpio, *Dalton Trans.* **2012**, *41*, 4634–4640.
[63] A. J. Tasiopoulos, T. A. O'Brien, K. A. Abboud, G. Christou, *Angew. Chem. Int. Ed.* **2004**, *43*, 345–349.
[64] A. J. Tasiopoulos, P. L. Milligan, K. A. Abboud, T. A. O'Brien, G. Christou, *Inorg. Chem.* **2007**, *46*, 9678–96791.
[65] Y.-J. Zhang, B.-Q. Ma, S. Gao, J.-R. Li, Q.-D. Liu, G.-H. Wen, X.-X. Zhang, *J. Chem. Soc. Dalt. Trans.* **2000**, 2249–2250.
[66] J. Liu, C. Ma, H. Chen, M. Hu, H. Wen, H. Cui, C. Chen, *Dalton Trans.* **2013**, *42*, 3787–3790.
[67] V. Chandrasekhar, A. Dey, S. Das, M. Rouzières, R. Clérac, *Inorg. Chem.* **2013**, *52*, 2588–2598.
[68] N. F. Chilton, R. P. Anderson, L. D. Turner, A. Soncini, K. S. Murray, *J. Comput. Chem.* **2013**, *34*, 1164–1175.
[69] A. Hosoi, Y. Yukawa, S. Igarashi, S. J. Teat, O. Roubeau, M. Evangelisti, E. Cremades, E. Ruiz, L. A. Barrios, G. Aromí, *Chem. Eur. J.* **2011**, *17*, 8264–8268.
[70] T. D. Pasatoiu, A. Ghirri, A. M. Madalan, M. Affronte, M. Andruh, *Dalton Trans.* **2014**, *43*, 9136–9142.
[71] S. J. Coles, P. A. Gale, *Chem. Sci.* **2012**, *3*, 683–689.
[72] G. M. Sheldrick, *Acta Crystallogr. Sect. C Struct. Chem.* **2015**, *71*, 3–8.
[73] A. L. Spek, *J. Appl. Crystallogr.* **2003**, *36*, 7–13.
[74] O. V. Dolomanov, L. J. Bourhis, R. J. Gildea, J. A. K. Howard, H. Puschmann, *J. Appl. Crystallogr.* **2009**, *42*, 339–341.
[75] L. J. Farrugia, *J. Appl. Crystallogr.* **2012**, *45*, 849–854.
[76] C. F. Macrae, P. R. Edgington, P. McCabe, E. Pidcock, G. P. Shields, R. Taylor, M. Towler, J. Van De Streek, *J. Appl. Crystallogr.* **2006**, *39*, 453–457.

FULL PAPER

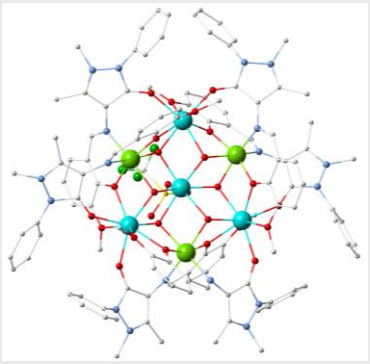

3d/4f coordination clusters

K. Griffiths, C. Harding, V. N. Dokorou, E. Loukopoulos, Stavroula I. Sampani, Alaa Abdul-Sada, G. J. Tizzard, Simon J. Coles, G. Lorusso, M. Evangelisti, A. Esquer and G. E. Kostakis**

Page No. – Page No.

Heptanuclear disk-like $M^{II}_3Ln^{III}_4$ (M=Ni,Co) coordination clusters: synthesis, structures and magnetic properties

The use of a monoanionic Schiff Base ligand in 3d/4f chemistry yields a family of heptanuclear $M^{II}_3Ln^{III}_4$ (M=Ni, Co) disk like coordination clusters. The Ni^{II}/Ln^{III} analogues represent the first examples bearing this disk-like topology. Magnetic studies reveal a dominant ferromagnetic coupling, while the $Ni^{II}_3Gd^{III}_4$ analogue **5** shows magnetocaloric properties at liquid-helium temperatures.